

## A STUDY ON MODELING OF RAT TUMORS WITH THE DISCRETE-TIME GOMPERTZ MODEL

Levent ÖZBEK

Department of Statistics, Faculty of Sciences, Ankara University, 06100 Ankara, TURKEY

**ABSTRACT.** Cancer formation is one of the pathologies whose frequency has increased in the recent years. In the literature, the compartment models, which are non-linear, are used for such problems. In nonlinear compartment models, nonlinear state space models and the extended Kalman filter (EKF) are used to estimate the parameter and the state vector. This paper presents a discrete-time Gompertz model (DTGM) for the transfer of optical contrast agent, namely indocyanine green (ICG), in the presence of tumors between the plasma and extracellular extravascular space (EES) compartments. The DTGM, which is proposed for ICG and the estimation of ICG densities used in the vascular invasion of tumor cells of the compartments and in the measurement of migration from the intravascular area to the tissues, is obtained from the experimental data of the study. The ICG values are estimated on-line (recursive) using the DTGM and the adaptive Kalman filter (AKF) based on the experimental data. By employing the data, the results show that the DTGM in conjunction with the AKF provides a good analysis tool for modeling the ICG in terms of mean square error (MSE), mean absolute percentage error (MAPE) and  $R^2$ . When the results obtained from the compartment model used in the reference [9] are compared with the results obtained with the DTGM, the DTGM gives better results in terms of MSE, MAPE and  $R^2$  criteria. The DTGM and the AKF compartment model require less numerical processing when compared to the EKF, which indicates that DTGM is a less complicated model. In the literature, EKF is used for such problems.

### 1. INTRODUCTION

In recent years the use of optical contrast agents and advanced medical imaging techniques to analyze and diagnose tissue abnormalities has become almost a standard procedure [1]. The existence of tumors is one of the main causes of tissue

---

2020 *Mathematics Subject Classification.* 62H12.

*Keywords.* Indocyanine green, tumor cell, discrete time Gompertz models, adaptive Kalman filter, estimation.

✉ ozbek@science.ankara.edu.tr; 0000-0003-1018-3114.

abnormalities, and in [2] it is shown that tumor vessel permeability to macromolecular blood solutes correlates with tumor growth as well as vascular growth. ICG is a blood pool agent that binds to globulin proteins (predominantly albumin) in blood [3], and because of its ability to bind to plasma proteins, it behaves as a macromolecular contrast agent with a low or no vascular permeability. Once injected, ICG rapidly and completely binds to albumin. Its macromolecular behavior results in a slow leakage which permits application of a pharmacokinetic model that in return allows for the determination of individual vascular parameters, such as capillary permeability. Compartmental analysis is a method of bio-mathematical modeling which assumes that a biological system can be divided into a series of homogeneous compartments which interact by exchanging material. For compartmental models used in pharmacokinetics, the material concentration varies with time depending on individual pharmacokinetics parameters [4]. If the appropriate parameters are known, the concentration level in a particular compartment can be predicted by applying suitable pharmacokinetic equations. Thus, a robust method of identifying and estimating individual parameters is required. The parameter identification is a common nonlinear estimation problem. In essence, it is the problem of estimating a model parameter that occurs as a coefficient of a dynamic system state variable - either as a dynamic coefficient or as measurement sensitivity. When this estimation problem is solved simultaneously with the state estimation problem (via state vector augmentation), the linear model becomes nonlinear. The extended Kalman filter (EKF) is one of the most popular and intensively investigated estimation technique for the nonlinear state estimation. It consists of applying the standard Kalman filter equations to the first-order approximation of the nonlinear model of the last estimate [5]. This study addresses the most commonly used growth models, the DTGM to estimate the ICG level without resorting to nonlinear models. The growth curves are used for modelling the increase in the number of plants, bacteria or viruses in an environment. The rest of this article is organized as follows. In Section 2, information about The ICG Compartment Model is presented. In Section 3, the mathematical and computational methodologies of DTGM are specified and the mathematical equations, that are aimed to be used further in the study are given, and the modeling analysis and estimation results are also presented. Finally, Section 4 concludes the study.

## 2. THE ICG COMPARTMENT MODEL

If there is a tumor in any tissue, the given ICG passes through the vessel into the tumor tissue area. There is also a return to the vein from the tumor tissue. In accordance with this physiological structure, a two-compartment model can be considered. In this compartment model,  $C_p$  indicates ICG concentration in the vessel,  $C_e$  indicates ICG concentration in tumor tissue.  $k_1$  ratio is the ratio of ICG passing from the vessel to the tumor tissue,  $k_2$  is the ratio of ICG passing from the tumor area into the vessel, and  $k_3$  is the ratio of ICG passing from the

plasma to the liver and kidney. Since the mentioned ratio is quite small, this ratio is ignored while creating the mathematical model. The ICG density in the tumor tissue tend to increase as the  $k_1$  ratio increase of the ICG density in the vessel (since there are transitions from here) and tend to decrease as the  $k_2$  ratio of its own density. Accordingly, the change in ICG density in the tumor tissue per unit time is expressed as in Equation 1,

$$\frac{dC_e(t)}{dt} = k_1 C_p(t) - k_2 C_e(t) \quad (1)$$

As mentioned above, its rate can be ignored, and the change in ICG density in the tumor tissue per unit time is defined as in Equation 2,

$$\frac{dC_p(t)}{dt} = -k_1 C_p(t) + k_2 C_e(t) \quad (2)$$

Because the ratio of ICG concentration, which is only in the vessel, is expected to be transferred to the tumor tissue per unit time.  $k_1$  and  $k_2$  show the permeability parameters mentioned before. According to the model, there is no information about the permeability parameters and there is no need for their estimates. When the differential equation system given by equations 1-2 are made discrete, nonlinear discrete time-state space model is obtained. In this model, both the parameter and the state vector are required to be estimated simultaneously. In the literature, the EKF is used for such problems [6]- [11].

### 3. DISCRETE-TIME GOMPertz MODEL

In this study, DTGM, one of the growth models, is used to estimate the ICG level without considering the nonlinear models.

The growth curves are used for modelling the increase in the number of plants, bacteria or viruses in an environment. Expressing the growth of an organism or an increase in the number of viruses temporally is called "growth". The identification of the complex growth process is aimed at using the growth curves [12]- [14]. DTGM is well known and widely used model in many sub-fields of biology [15]- [18]. Numerous parametrizations and re-parametrizations of the DTGM can be found in the literature [17]. DTGM was originally recommended to explain human mortality curves Gompertz [12], and it has been further used in the description of growth processes, for example, growing of bacterial colonies [15] and tumors [16]. The model, a stochastic version of the DTGM, can be transformed into a linear Gaussian state-space model for the convenient fitting to time-series data. In this study, ICG values are estimated online using the DTGM and the AKF based on the experimental data. By employing the data, the results show that the DTGM in conjunction with AKF provides a good analysis tool for modeling the ICG in terms of mean square error (MSE), mean absolute percentage error (MAPE), and  $R^2$ . When the results obtained from the compartment model used in the reference [9] are compared with the results obtained with the DTGM, the DTGM gives

better results in terms of MSE, MAPE and  $R^2$  criteria. The DTGM and the AKF compartment model require less numerical processing when compared to the EKF, which indicates that DTGM is a less complicated model.

Let  $n_t$  denote ICG level at time  $t$ . The process model is as:

$$n_t = n_{t-1} \exp(a + b \ln n_{t-1} + e_t) \quad (3)$$

where  $a$  and  $b$  are constants, and  $e_t$  is a random variable distributed as  $e_t \sim N(0, \sigma_1^2)$ . The random variables  $e_1, \dots, e_n$  are assumed to be uncorrelated. On the logarithmic scale, the DTGM is a linear autoregressive time-series model of order 1 [AR(1) process] defined as equation 4.

$$y_t = y_{t-1} + a + b y_{t-1} + e_t = a + c y_{t-1} + e_t \quad (4)$$

where,  $y_t = \ln n_t$  and  $c = b + 1$ . For statistical properties of DTGM, see [18].

The model has a long history in density-dependence modeling see [19]- [21]. A frequently seen alternative is a stochastic version of the Moran-Ricker model [21], which uses  $n_{t-1}$  instead of  $\ln n_{t-1}$  in the exponential function; in comparative data analysis studies, the Gompertz model has performed as well as the Moran-Ricker [22]. The probability distribution of  $n_{t-1}$  is a normal distribution with mean and variance that change as functions of time. If  $-1 < c < 1$ , the probability distribution of  $n_t$  eventually approaches a time-independent stationary distribution that is a normal distribution with a mean of  $a/(1-c)$  and a variance of  $\sigma_1^2/(1-c^2)$ . The stationary distribution is the stochastic version of an equilibrium in the deterministic model, and is an important statistical manifestation of density dependence in the population growth model Dennis [18]. In equation 4,  $a$  is the intrinsic growth rate,  $b$  is the density-dependent influence [18].

**3.1. Mathematical and Computational Methodologies.** The optimum linear filtering and estimation methods introduced by Kalman [31] have been considered as one of the greatest achievements in estimation theory. Discrete-time linear state-space models and Kalman filtering (KF) have been employed since the 1960s, mostly in the control and signal processing areas. The KF has been extensively employed in many areas of estimation. The extensions and applications of discrete-time linear state-space models can be found in almost all disciplines [20]- [28]. In this study, KF has been used to estimate the time-varying parameter of the DTGM. KF is a recursive estimator to estimate the time-varying parameters. If  $a = 0$  in Eq.(4),  $n_t$  takes the case counts observed until  $t$  and  $y_t = \ln n_t$ . Then the equation

$$y_t = c y_{t-1} + e_t \quad (5)$$

is acquired. In the case that the parameter  $c$  in Eq.(5) is time-varying and presumed as random walk process, that is . Then state-space model,

$$y_t = c_t y_{t-1} + e_t \quad (6)$$

$$c_t = c_{t-1} + w_t \quad (7)$$

is obtained and  $w_t$  is distributed as  $w_t N(0, \sigma_2^2)$ . The random variables  $w_1, w_2, \dots, w_n$  are assumed to be uncorrelated. Here, the state variable is unobservable, time-varying, and can be estimated through AKF (explanation regarding AKF is given in the Appendix section). If this time-varying parameter is estimated using on-line AKF, the ICG level in times  $t+1, t+2, \dots$  can be estimated via this online-estimated parameter. When the models given in equations (6) and (7) are compared with the state space model given in the Appendix, the following equations are obtained.

$$x_t = c_t, F_t = 1, G_t = 1, H_t = y_{t-1}, R_t = \sigma_1, Q_t = \sigma_2 \quad (8)$$

**3.2. Application of DTGM.** Details of the experimental setup, and how the data were collected can be found in [23]. Data is given in Table 1. Since this study deals with the collected data, here only a very brief discussion regarding the experiments is given in order to put more emphasis on the mathematical representation, along with parameter estimation. In the experiments, bolus injections of the optical contrast agent ICG were administered to the rat through the tail vein. The measurements were collected by placing the probe normal to the tumor surface and probing the whole tissue including plasma. After injection, ICG rapidly and completely binds to albumin, after which the kinetics of ICG are governed by the temporal dynamics of albumin in and between the vascular compartment and the EES.

**3.3. Estimation (AKF) Algorithm.** The steps of the AKF algorithm using to estimate the parameter in DTGM are as follows. The code is written in Matlab program for the estimation algorithm.

Step 1. Initial values  $\hat{c}_0 = 0.9, P_0 = 1, R_t = \sigma_1 = \text{std}(y_t), t = 1, 2, \dots, n, Q_t = \sigma_2 = 0.01, t = 1, 2, \dots, n, \alpha = 1.0001$

Step 2.  $\hat{c}_{t|t-1} = \hat{c}_{t-1}$  Predicted (a priori) state estimate

Step 3.  $P_{t|t-1} = \alpha(P_{t-1t-1} + \sigma_2)$  Predicted (a priori) estimate covariance

Step 4.  $K_t = P_{t|t-1}y_{t-1} (y_{t-1}P_{t|t-1}y_{t-1} + \sigma_1)^{-1}$  Optimal Kalman gain

Step 5.  $P_{t=} = [I - K_t y_{t-1}] P_{t|t-1}$  Updated (a posteriori) estimate covariance

Step 6.  $\hat{c}_t = \hat{c}_{t|t-1} + K_t (y_t - y_{t-1}\hat{c}_{t|t-1})$  Updated (a posteriori) state estimate

In the experiment, the ICG concentration in the lump space, i.e. EES and plasma, was monitored for 500 seconds. According to the estimation results obtained by using the ICG level in DTGM, the MSE, MAPE,  $R^2$  and values are calculated (see Table 2). These calculated values indicate that the compatibility of the model with real data is quite high. This tells us estimating the ICG level via DTGM is a reliable method. Since estimation using the AR(1) stochastic process does not require any other model assumption. As for AKF, utilizing only the observation in time and the preceding estimation is the most advantageous aspect of this method.

TABLE 1. Collected data.

Time	Observed value										
0	-0.0237	45	0.623	90	0.749	135	0.682	180	0.603	225	0.532
1	-0.0269	46	0.632	91	0.752	136	0.677	181	0.596	226	0.533
2	-0.0282	47	0.645	92	0.753	137	0.678	182	0.594	227	0.534
3	-0.0251	48	0.65	93	0.751	138	0.683	183	0.594	228	0.533
4	-0.0249	49	0.66	94	0.747	139	0.684	184	0.591	229	0.527
5	-0.0224	50	0.665	95	0.739	140	0.685	185	0.592	230	0.531
6	-0.0236	51	0.671	96	0.741	141	0.688	186	0.586	231	0.528
7	-0.0243	52	0.682	97	0.743	142	0.686	187	0.587	232	0.527
8	-0.0232	53	0.685	98	0.748	143	0.688	188	0.591	233	0.525
9	0.0265	54	0.688	99	0.747	144	0.685	189	0.594	234	0.521
10	0.139	55	0.688	100	0.742	145	0.671	190	0.587	235	0.523
11	0.216	56	0.691	101	0.739	146	0.661	191	0.579	236	0.523
12	0.255	57	0.696	102	0.741	147	0.657	192	0.576	237	0.522
13	0.275	58	0.704	103	0.738	148	0.66	193	0.579	238	0.514
14	0.282	59	0.711	104	0.738	149	0.662	194	0.576	239	0.513
15	0.286	60	0.716	105	0.738	150	0.658	195	0.575	240	0.516
16	0.295	61	0.717	106	0.735	151	0.653	196	0.574	241	0.513
17	0.305	62	0.729	107	0.739	152	0.652	197	0.574	242	0.508
18	0.316	63	0.737	108	0.739	153	0.654	198	0.573	243	0.503
19	0.324	64	0.739	109	0.731	154	0.653	199	0.572	244	0.504
20	0.337	65	0.729	110	0.734	155	0.653	200	0.57	245	0.502
21	0.352	66	0.725	111	0.734	156	0.646	201	0.568	246	0.504
22	0.365	67	0.726	112	0.737	157	0.648	202	0.567	247	0.503
23	0.381	68	0.732	113	0.733	158	0.654	203	0.569	248	0.503
24	0.399	69	0.728	114	0.734	159	0.652	204	0.566	249	0.497
25	0.413	70	0.722	115	0.736	160	0.645	205	0.566	250	0.5
26	0.426	71	0.725	116	0.727	161	0.639	206	0.566	251	0.5
27	0.439	72	0.732	117	0.724	162	0.635	207	0.565	252	0.501
28	0.45	73	0.731	118	0.723	163	0.631	208	0.568	253	0.5
29	0.466	74	0.731	119	0.719	164	0.629	209	0.564	254	0.504
30	0.477	75	0.732	120	0.718	165	0.623	210	0.557	255	0.501
31	0.49	76	0.736	121	0.711	166	0.62	211	0.553	256	0.499
32	0.503	77	0.74	122	0.699	167	0.62	212	0.551	257	0.491
33	0.513	78	0.738	123	0.702	168	0.623	213	0.554	258	0.489
34	0.524	79	0.743	124	0.699	169	0.623	214	0.546	259	0.486
35	0.537	80	0.743	125	0.7	170	0.622	215	0.543	260	0.49
36	0.553	81	0.751	126	0.699	171	0.621	216	0.54	261	0.486
37	0.569	82	0.755	127	0.697	172	0.62	217	0.541	262	0.482
38	0.579	83	0.756	128	0.696	173	0.623	218	0.538	263	0.478
39	0.579	84	0.754	129	0.702	174	0.626	219	0.538	264	0.477
40	0.58	85	0.747	130	0.697	175	0.624	220	0.537	265	0.477
41	0.589	86	0.747	131	0.691	176	0.617	221	0.535	266	0.476
42	0.597	87	0.749	132	0.684	177	0.608	222	0.537	267	0.477
43	0.605	88	0.749	133	0.681	178	0.609	223	0.532	268	0.479
44	0.613	89	0.745	134	0.679	179	0.607	224	0.531	269	0.476
270	0.48	315	0.441	360	0.419	405	0.396	450	0.382	495	0.374
271	0.478	316	0.438	361	0.417	406	0.395	451	0.378	496	0.377
272	0.477	317	0.437	362	0.414	407	0.397	452	0.381	497	0.375
273	0.474	318	0.437	363	0.409	408	0.396	453	0.383	498	0.374
274	0.471	319	0.438	364	0.409	409	0.395	454	0.381	499	0.376
275	0.474	320	0.441	365	0.409	410	0.396	455	0.381	500	0.372
276	0.473	321	0.437	366	0.409	411	0.397	456	0.383	501	0.371
277	0.471	322	0.434	367	0.407	412	0.396	457	0.382	502	0.369
278	0.467	323	0.433	368	0.405	413	0.391	458	0.383	503	0.368
279	0.468	324	0.434	369	0.408	414	0.391	459	0.38	504	0.37
280	0.467	325	0.432	370	0.407	415	0.389	460	0.382		
281	0.464	326	0.433	371	0.406	416	0.391	461	0.378		
282	0.468	327	0.43	372	0.408	417	0.391	462	0.376		
283	0.462	328	0.43	373	0.409	418	0.391	463	0.38		
284	0.465	329	0.429	374	0.411	419	0.393	464	0.379		
285	0.465	330	0.432	375	0.405	420	0.394	465	0.379		
286	0.463	331	0.433	376	0.407	421	0.392	466	0.377		
287	0.462	332	0.434	377	0.409	422	0.393	467	0.376		
288	0.46	333	0.429	378	0.406	423	0.396	468	0.376		
289	0.462	334	0.427	379	0.407	424	0.393	469	0.378		
290	0.465	335	0.423	380	0.408	425	0.395	470	0.377		
291	0.461	336	0.423	381	0.407	426	0.391	471	0.379		
292	0.454	337	0.422	382	0.41	427	0.392	472	0.383		
293	0.452	338	0.424	383	0.406	428	0.389	473	0.38		
294	0.45	339	0.421	384	0.4	429	0.391	474	0.38		
295	0.452	340	0.423	385	0.396	430	0.387	475	0.378		
296	0.448	341	0.421	386	0.398	431	0.39	476	0.378		
297	0.45	342	0.418	387	0.399	432	0.391	477	0.38		
298	0.447	343	0.418	388	0.395	433	0.388	478	0.378		
299	0.446	344	0.419	389	0.393	434	0.384	479	0.377		
300	0.448	345	0.417	390	0.394	435	0.387	480	0.372		
301	0.442	346	0.419	391	0.393	436	0.385	481	0.373		
302	0.448	347	0.415	392	0.392	437	0.385	482	0.373		
303	0.447	348	0.419	393	0.397	438	0.386	483	0.372		
304	0.447	349	0.42	394	0.395	439	0.387	484	0.375		
305	0.446	350	0.419	395	0.398	440	0.388	485	0.374		
306	0.449	351	0.417	396	0.397	441	0.39	486	0.375		
307	0.447	352	0.416	397	0.395	442	0.389	487	0.373		
308	0.443	353	0.418	398	0.395	443	0.388	488	0.374		
309	0.441	354	0.416	399	0.397	444	0.387	489	0.375		
310	0.441	355	0.415	400	0.395	445	0.386	490	0.373		
311	0.437	356	0.417	401	0.397	446	0.384	491	0.374		
312	0.44	357	0.418	402	0.395	447	0.382	492	0.374		
313	0.439	358	0.417	403	0.394	448	0.382	493	0.375		
314	0.438	359	0.418	404	0.395	449	0.384	494	0.376		

TABLE 2. Calculated  $R^2$ , MSE, MAPE.

Model	MSE	$R^2$	MAPE
DTGM	0.0001	0.9973	5.7385
Compartment Models	0.0004	0.9826	19.2059

Figure 1 depicts the observed ICG concentration and the model fit obtained through the use of DTGM. Figure 2 depicts the observed ICG concentration and the model fit obtained through the use of compartment models [9]. Figure 3 depicts the observed ICG concentration and the model fit obtained through the use of compartment models and DTGM. It is clearly seen that the DTGM mathematical model provides a rather good fit to the observations, which indicates the correctness of the model.

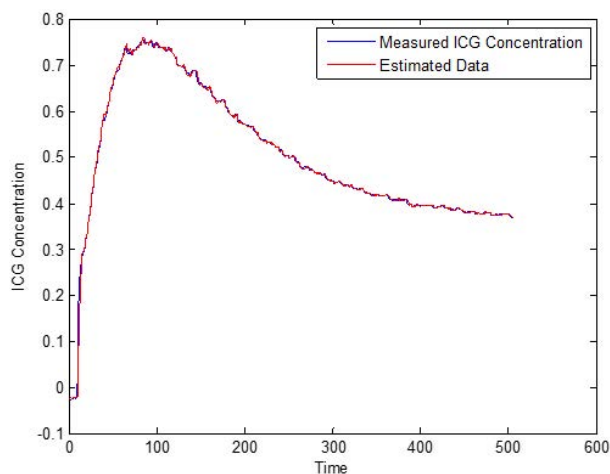


FIGURE 1. DTGM: Observed ICG concentration and the model fit.

#### 4. CONCLUSION

In this study, we introduced a DTGM representing the metabolic elimination and transfer of ICG between compartments in rat tumors, and presented a method for the quantitative analysis of experimentally obtained ICG concentration data. This will be useful in the analysis of tumor cell behavior patterns in cancerous tissues. In this study, ICG concentration data have been estimated online using DTGM and AKF. The ICG concentration data is modeled with DTGM, and the time-varying parameters of the obtained AR(1) stochastic time series are estimated

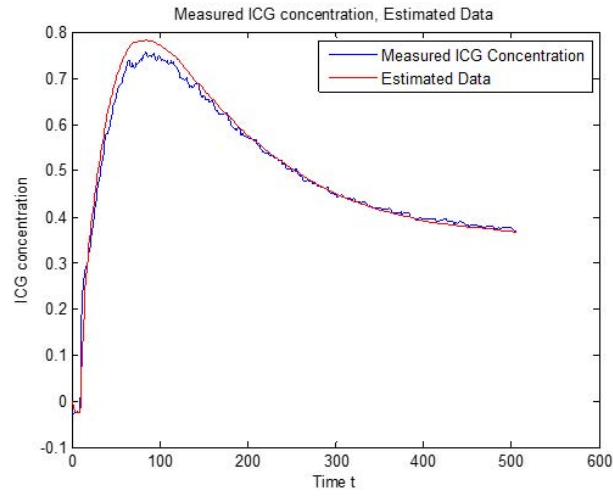


FIGURE 2. Compartment Models: Observed ICG concentration and the model fit.

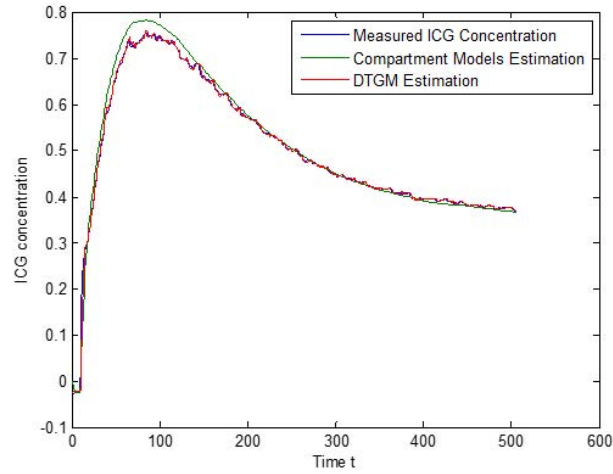


FIGURE 3. Compartment Models and DTGM: Observed ICG concentration and the model fit.

by the on-line AKF. The estimation by the acquired data shows that employing the DTGM model and the AKF in terms of MSE, MAPE, and  $R^2$  provide efficient

analysis for modeling the ICG concentration data. It is proposed that using the DTGM and the AKF will be appropriate. It is quite a simple method to model the ICG concentration time series data with the time-varying parameter AR(1) stochastic process and to estimate the time-varying parameter with the online AKF. When the results obtained from the compartment model used in the reference [9] are compared with the results obtained with the DTGM, the DTGM offers better results according to MSE, MAPE and  $R^2$  criteria. The DTGM and the AKF compartment model require less numerical processing compared to the EKF, and DTGM is a simpler model. In the literature, the EKF is used for such problems. As far as we know no other method has been used before.

**Appendix**

**State-Space Model and Adaptive Kalman Filter (AKF)**

Let us consider a general discrete-time stochastic system represented by the state and measurement models given as:

$$\begin{aligned} x_{t+1} &= F_t x_t + G_t w_t \\ y_t &= H_t x_t + v_t \end{aligned}$$

where  $x_t$  is an  $n \times 1$  system vector,  $y_t$  is an  $m \times 1$  observation vector,  $F_t$  is an  $n \times n$  system matrix,  $H_t$  is an  $m \times n$  matrix,  $w_t$  an  $n \times 1$  vector of zero mean white noise sequence and  $v_t$  is an  $m \times 1$  measurement error vector assumed to be a zero mean white sequence uncorrelated with the  $w_t$  sequence. The covariance matrices  $w_t$  and  $v_t$  are defined by  $w_t \sim N(0, Q_t)$ ,  $v_t \sim N(0, R_t)$ . The filtering problem is the problem of determining the best estimate of its  $x_t$  condition, given its observations  $Y_t = (y_0, y_1, \dots, y_t)$  [14–20]. When  $Y_t = (y_0, y_1, \dots, y_t)$  observations are given, the estimation of state  $x_t$  with

$$\hat{x}_t = E(x_t | y_0, y_1, \dots, y_t) = E(x_t | Y_t)$$

and the covariance matrix of the error with

$$P_{t|t} = E[(x_t - \hat{x}_{t|t})(x_t - \hat{x}_{t|t})' | Y_t]$$

when  $Y_{t-1} = (y_0, y_1, \dots, y_{t-1})$  observations are given, the estimation of state  $x_t$  with  $\hat{x}_{t|t-1} = E(x_t | y_0, y_1, \dots, y_{t-1}) = E(x_t | Y_{t-1})$

and the covariance matrix of the error are shown with

$$P_{t|t-1} = E[(x_t - \hat{x}_{t|t-1})(x_t - \hat{x}_{t|t-1})' | Y_{t-1}].$$

Let the initial state be assumed to have a normal distribution in the form of  $x_0 \sim N(\bar{x}_0, P_0)$ .

The optimum update equations for KF are,

$$\hat{x}_{t|t-1} = F_{t-1} \hat{x}_{t-1}$$

$$P_{t|t-1} = F_{t-1} P_{t-1} F_{t-1}' + G_{t-1} Q_{t-1} G_{t-1}'$$

$$K_t = P_{t|t-1}H_t'(H_tP_{t|t-1}H_t' + R_t)^{-1}$$

$$P_{t|t} = [I - K_tH_t]P_{t|t-1}$$

$$\hat{x}_t = \hat{x}_{t|t-1} + K_t(y_t - H_t\hat{x}_{t|t-1})$$

In the above equations,  $\hat{X}_{t|t-1}$  is the a priori estimation and  $\hat{X}_t$  is the a posteriori estimation of  $x_t$ . Also,  $P_{t|t-1}$  and  $P_{t|t}$  are the covariance of a priori and a posteriori estimations respectively [24]- [33]. In some cases, divergence problems may occur in the KF due to the incorrect installation of the model. In order to eliminate divergence in the KF, adaptive methods are used [5], [32], [33]. One of these is the use of the forgetting factor. A forgetting factor is proposed by [32].

$$P_{t|t-1} = \alpha (F_{t-1}P_{t-1|t-1}F_{t-1}' + G_{t-1}Q_{t-1}G_{t-1}')$$

**Declaration of Competing Interests** The author declare that there is no conflict of interest regarding the publication of this article.

#### REFERENCES

- [1] Tofts, P.S., Modeling tracer kinetics in dynamic Gd-DTPA MR imaging, *J. Magn. Reson. Imag.*, 7 (1997), 91-101. doi: 10.1002/jmri.1880070113
- [2] Su, M.Y., Jao, J.C., Nalcioğlu, O., Measurement of vascular volume fraction and blood-tissue permeability constants with a pharmacokinetic model: studies in rat muscle tumors with dynamic Gd-DTPA enhanced MRI, *Magn. Reson. Med.*, 32 (1994), 714-724. doi: 10.1002/mrm.1910320606
- [3] Ntziachristos, V., Yodh, A.G., Schnall, M., Chance, B., Concurrent MRI and diffuse optical tomography of breast after indocyanine green enhancement, *Proc. Natl. Acad. Sci. USA*, 97 (2000), 2767-2772. doi/10.1073/pnas.040570597
- [4] Botsman, K., Tickle, K., Smith, J.D., A Bayesian formulation of the Kalman filter applied to the estimation of individual pharmacokinetic parameters, *Comput. Biomed. Res.*, 30 (1997), 83-93. doi/10.1006/cbmr.1997.1440
- [5] Özbek, L., Efe, M., An adaptive extended Kalman filter with application to compartment models, *Communications In Statistics-Simulation and Computation*, 33(1) (2004), 145-158. doi/10.1081/SAC-120028438
- [6] Alacam, B., Yazici, B., Chance, B., Extended Kalman filtering for the modeling and analysis of ICG pharmacokinetics in cancerous tumors using NIR optical methods, *IEEE Transactions on Biomedical Engineering*, 53(10) (2006), 1861-1871. doi:10.1109/TBME.2006.881796
- [7] Alacam, B., Yazici, B., Intes, X., Nioka, S., Chance, B., Pharmacokinetic-rate images of indocyanine green for breast tumors using near-infrared optical methods, *Phys. Med. Biol.*, 53 (2008), 837-859. doi: 10.1088/0031-9155/53/4/002
- [8] Alacam, B., Yazici, B., Direct reconstruction of pharmacokinetic-rate images of optical fluorophores from NIR measurements, *IEEE Transactions on Medical Imaging*, 28(9) (2009), 1337-1353. doi: 10.1109/TMI.2009.2015294
- [9] Özbek, L., Efe, M., Babacan, E.K., Yazihan, N., Online estimation of capillary permeability and contrast agent concentration in rat tumors, *Hacettepe Journal of Mathematics and Statistics*, 39(2) (2010), 283-293.

- [10] Gottam, O., Naik, N., Gambhirc, S., Parameterized level-set based pharmacokinetic fluorescence optical tomography using the regularized Gauss-Newton filter, *Journal of Biomedical Optics*, 24(3) (2019), 1-17. doi/10.1117/1.JBO.24.3.031010
- [11] Gottam, O., Naik, N., Gambhirc, S., Pandey, P.K., RBF level-set based fully-nonlinear fluorescence photoacoustic pharmacokinetic tomography, *Inverse Problems in Science and Engineering*, doi/10.1080/17415977.2021.1982934
- [12] Gompertz, B., On the nature of the function expressive of the law of human mortality, and on a new mode of determining the value of life contingencies, *Philosophical Transactions of the Royal Society of London*, 115 (1825), 513-583.
- [13] Bertalanffy, L., Problems of organic growth, *Nature*, 163 (1949), 156-158.
- [14] Richards, F.A., Flexible growth function for empirical use, *Journal of Experimental Botany*, 10 (1959), 280-300.
- [15] Zwietering, M.H., Jongenburger, I., Rombouts, F.M., Van't Riet, K., Modeling of the bacterial growth curve, *Appl Environ Microbiol*, 56(6) (1990), 1875-1881. doi: 10.1128/aem.56.6.1875-1881.1990
- [16] Gerlee, P., The model muddle: in search of tumor growth laws, *Cancer research*, 73(8) (2013), 2407-2411. doi/10.1158/0008-5472.CAN-12-4355
- [17] Tjorve, K.M.C., Tjorve, E., The use of Gompertz models in growth analyses, and new Gompertz-model approach: An addition to the Unified-Richards family, *PLoS One*, 12(6) (2017), e0178691. doi/10.1371/journal.pone.0178691
- [18] Dennis, B., Ponciano, J.M., Subhash, R., Traper, L.M.L., Staples, D.F., Estimating density dependence, process noise and observation errors, *Ecological Monographs*, 76(3) (2006), 323-341. doi/10.1890/0012-9615.
- [19] Reddingius, J., Gambling for existence: A discussion of some theoretical problems in animal population ecology, *Acta Biotheoretica*, 20 (1971), 1-208.
- [20] Pollard, E., Lakhani, K.H., Rothery, P., The detection of density-dependence from a series of annual censuses, *Ecology*, 68 (1987), 2046-2055. doi: 10.2307/1939895
- [21] Dennis, B., Taper, M.L., Density dependence in time series observations of natural populations: estimation and testing, *Ecological Monographs*, 64 (1994), 205-224. doi/10.2307/2937041
- [22] Rotella, J.J., Ratti, J.T., Reese, K.P., Taper, M.L., Dennis, B., Long-term population analysis of Gray Partridge in eastern Washington, *Journal of Wildlife Management*, 60 (1996), 817-825. doi/10.2307/3802382
- [23] Cuccia, D.J., Bevilacqua, F., Durkin, A.J., Merritt, S., Tromberg, B.J., Gulsen, G., Yu, H., Wang, J., Nalcioglu, O., In vivo quantification of optical contrast agent dynamics in rat tumors by use of diffuse optical spectroscopy with magnetic resonance imaging coregistration, *Appl. Opt.*, 42 (2003), 2940-2950. doi/10.1364/AO.42.002940
- [24] Jazwinski, A.H., *Stochastic Processes and Filtering Theory*, Academic Press, 1970.
- [25] Anderson, B.D.O., Moore, J.B., *Optimal Filtering*, Prentice Hall, 1979.
- [26] Chui, C.K., Chen, G., *Kalman Filtering with Real-time Applications*, Springer Verlag, 1991.
- [27] Ljung, L., Söderström T., *Theory and Practice of Recursive Identification*, The MIT Press, 1993.
- [28] Chen, G., *Approximate Kalman Filtering*, World Scientific, 1993.
- [29] Grewal, S.M., Andrews, A.P., *Kalman Filtering: Theory and Practice*, Prentice Hall, 1993.
- [30] Özbek, L., *Kalman Filtresi*, Akademisyen Kitabevi, 2017.
- [31] Kalman, R.E., A new approach to linear filtering and prediction problems, *Journal of Basic Engineering*, 82 (1960), 35-45. <http://dx.doi.org/10.1115/1.3662552>
- [32] Özbek, L., Aliev, F.A., Comments on adaptive Fading Kalman filter with an application, *Automatica*, 34(12) (1998), 1663-1664.
- [33] Efe, M., Özbek, L., Fading Kalman filter for manoeuvring target tracking, *Journal of the Turkish Statistical Association*, 2(3) (1999), 193-206.